UC DAVIS
UNIVERSITY OF CALIFORNIA

ASU ARIZONA STATE UNIVERSITY

Toward Topological Spintronics:

Local Conductance on Terraced Bi_2Te_3 Surfaces and Proximity Induced Ferromagnetism from Nanoparticle Arrays

Richard A. Kiehl

Electrical, Computer and Energy Engineering

Arizona State University

Surface Topography of MBE Grown Bi_2Te_3

AFM Image

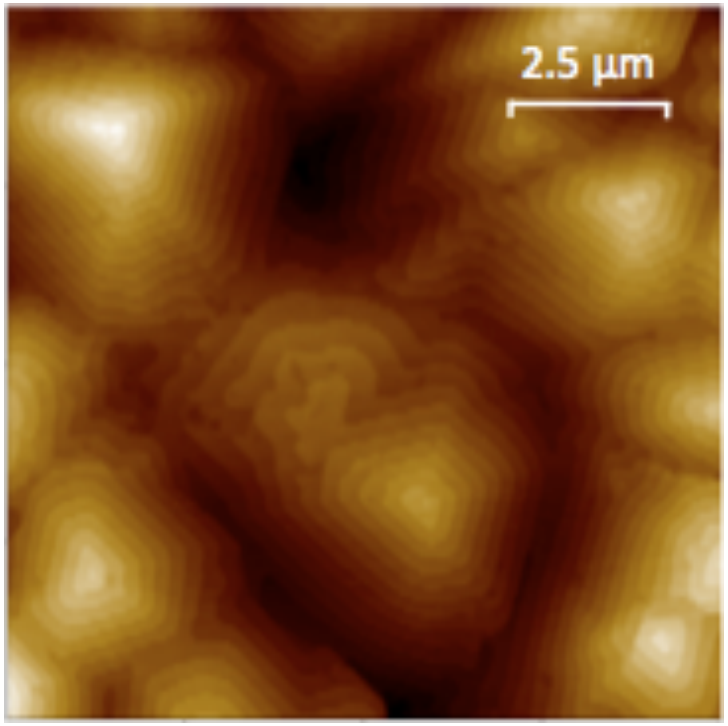

Triangular Quintuple-Layer Terraces
1 nm Steps, 200 nm Ledges

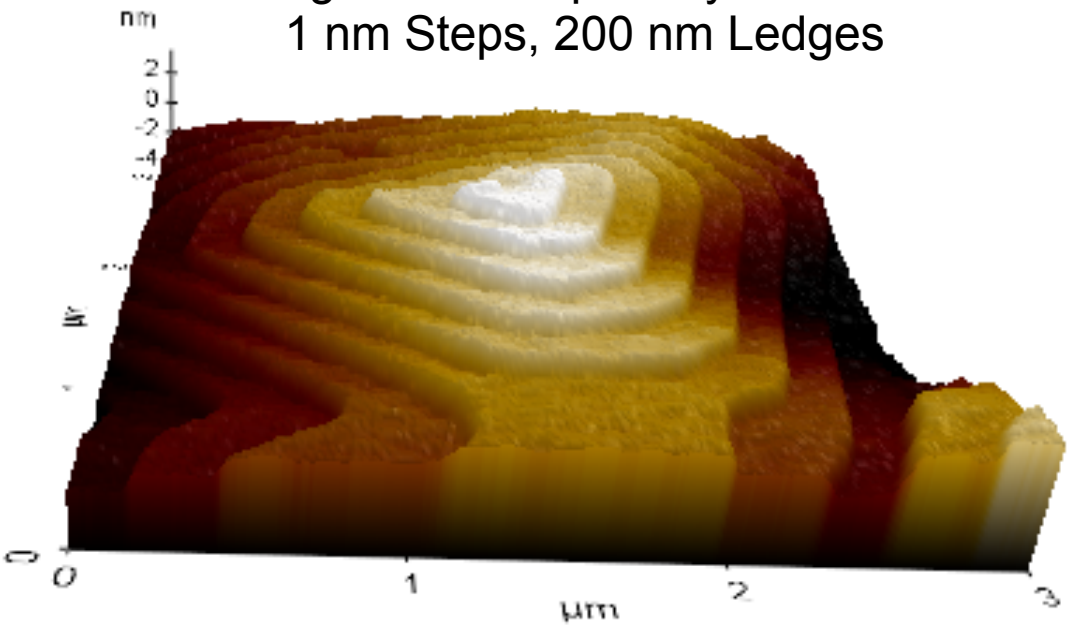

Room Temperature Ambient Environment

10-100X Enhancement of Conductance at Terrace Step Edges

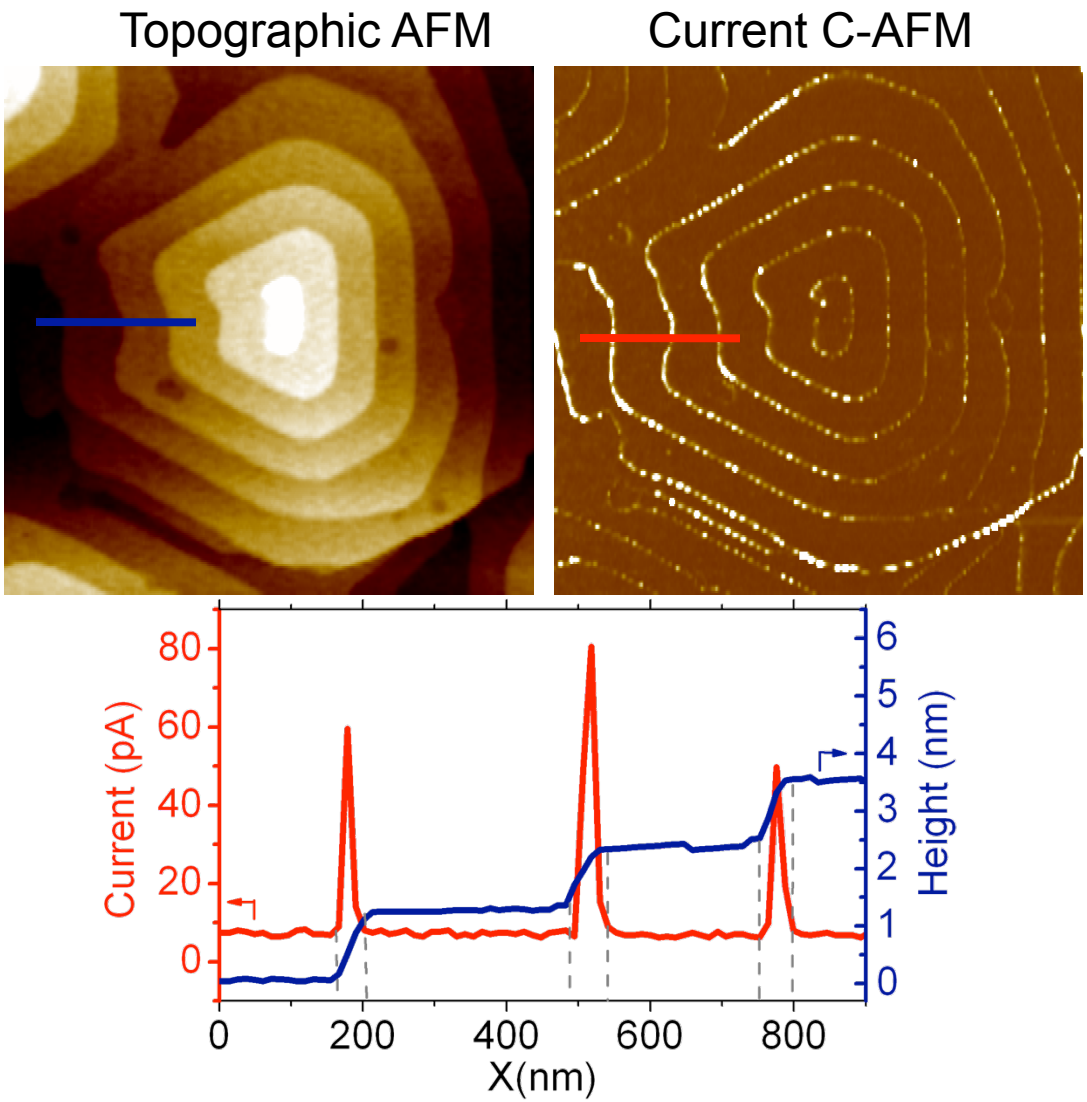

Geometric Tip Artifact?

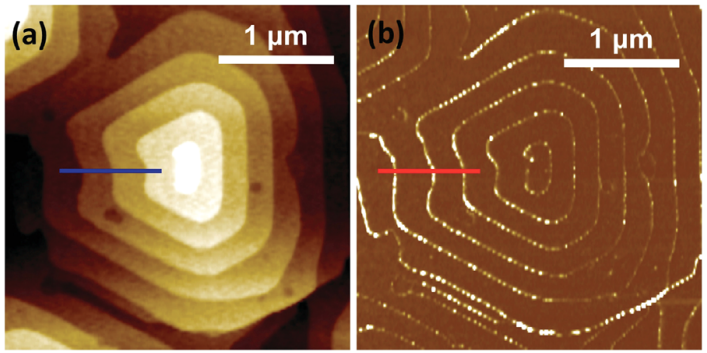

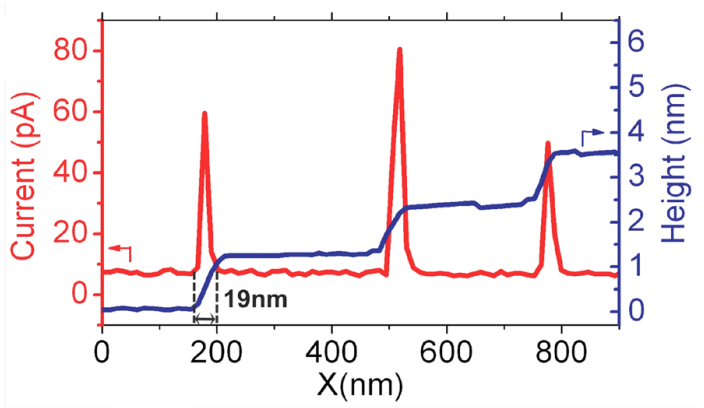

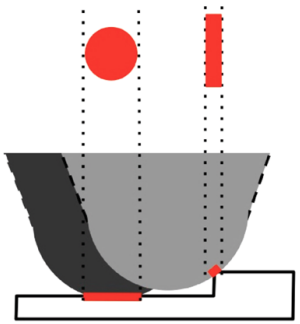

Control Sample #1 - Nanoparticles

- Typical AFM topography and corresponding C-AFM images of Fe_3O_4 NPs on graphene
  - NPs nominal Ø~17 nm
  - ΔI~21% (over a Δw~10nm)

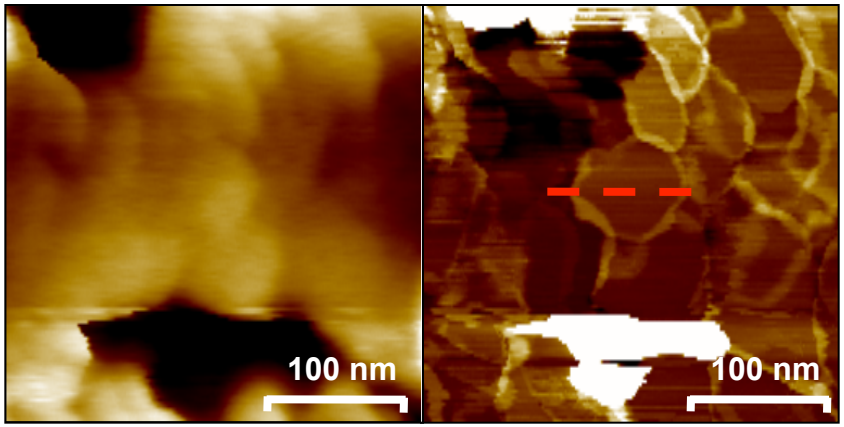

Dia_{app}^{NPs} ~ 83 nm

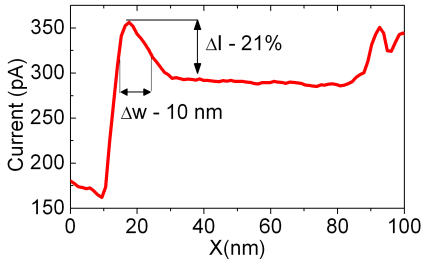

- Model of tip-sample interaction for a sample comprising spheres
  - Allows to estimate "real" tip radius using the apparent width of NPs on AFM image

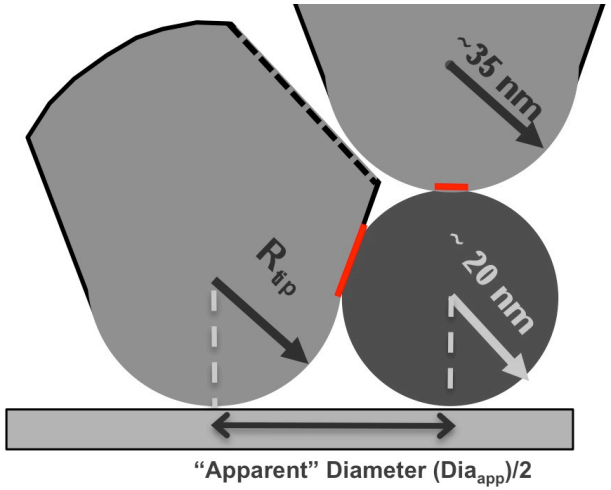

$$Dia_{app} = 4\sqrt{R_{tip}R_{NP}}$$

Dia_{app} NPs	R_{tip}
83 nm	51 nm

Control Sample #2 - HOPG

- Typical AFM topography and corresponding C-AFM images of an HOPG sample.
  - Monolayers: Δh~0.25 nm ➔ΔI~17% (over a Δw~12nm)
  - Multilayers: Δh~1 nm ➔ΔI~25% (over a Δw~10nm)

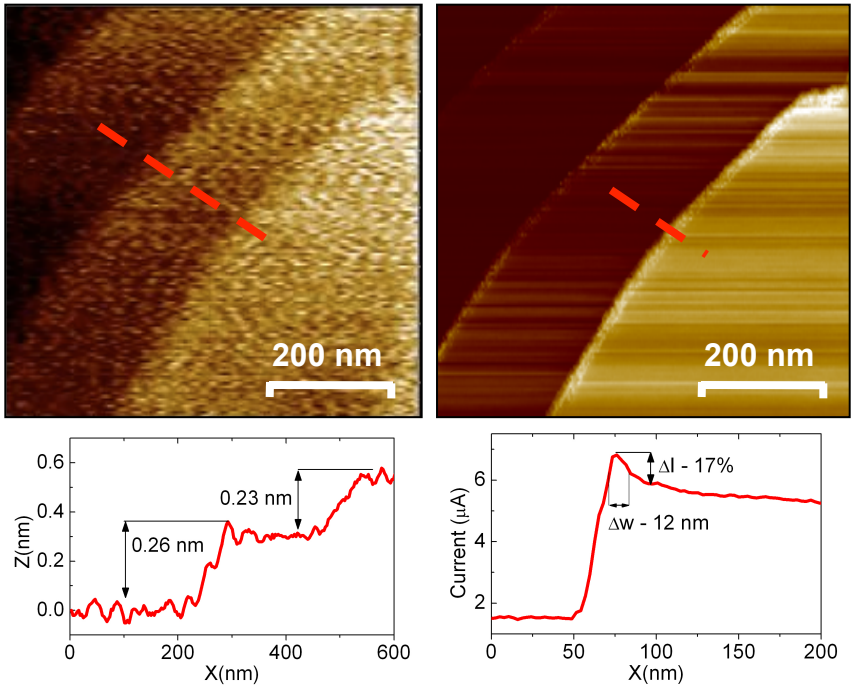

- Model of tip-sample interaction for terraced structures

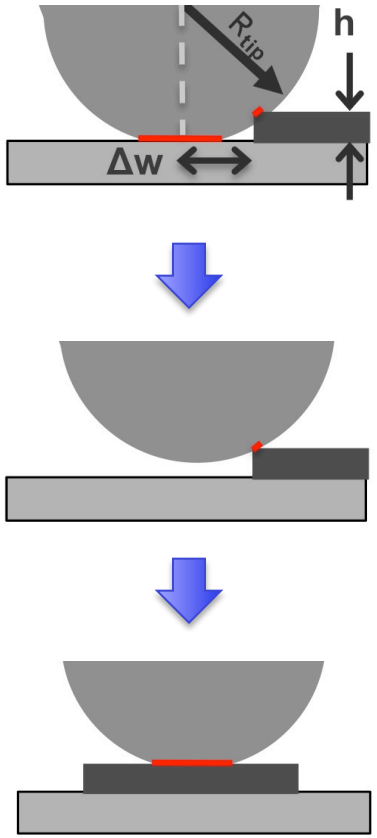

  - Allows to estimate width of high current regions

$$\Delta w = \sqrt{h\left(2R_{tip} - h\right)}$$

Assuming tip radius =50nm

	BiTe h~1nm	HOPG h~0.25nm
Δw measured	19.02 ±5.74 nm	10 nm
Δw estimated	7.2 ±5.3 nm	5 nm

Effects of Scan Direction and Sample Rotation

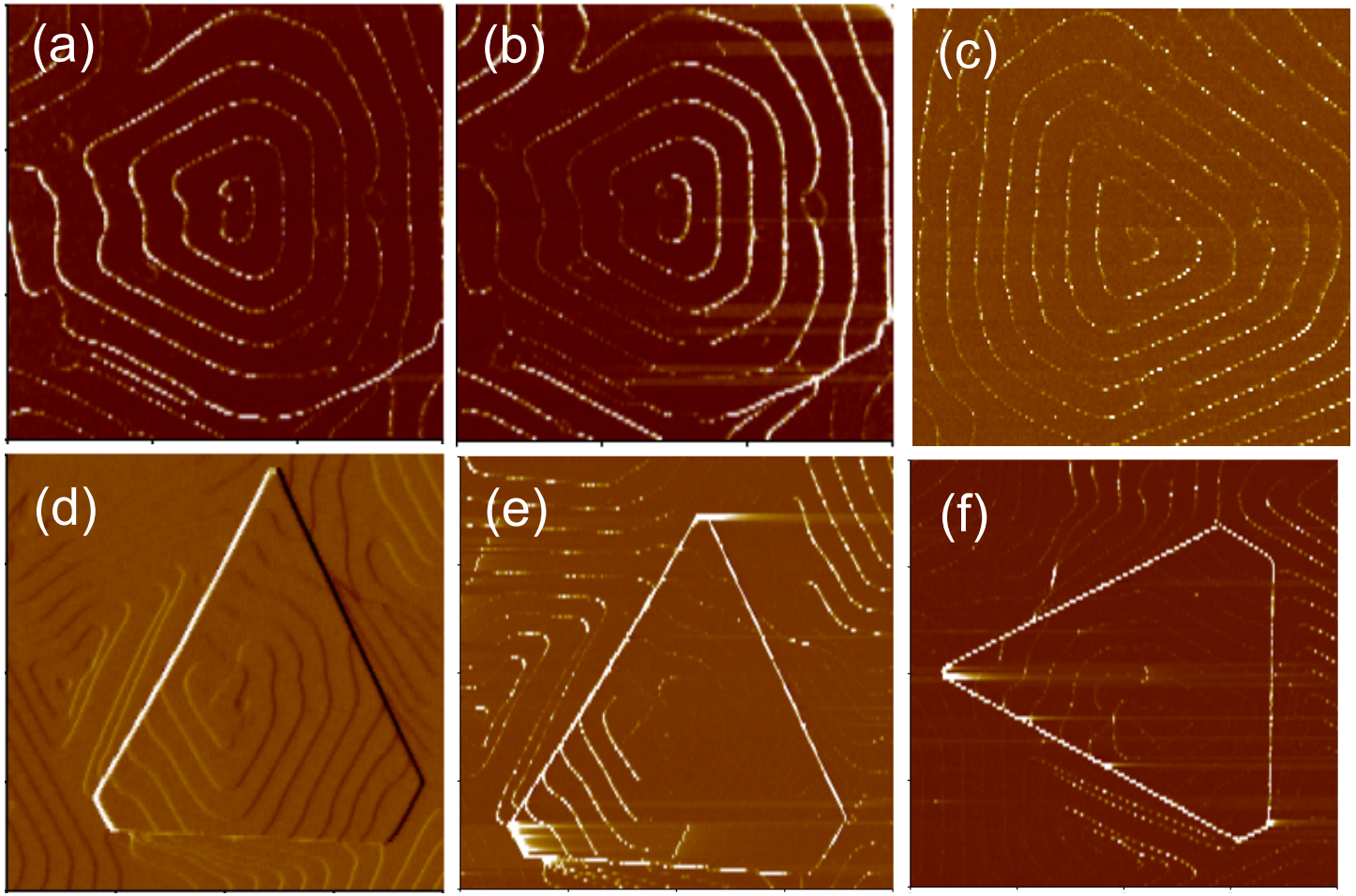

Fixed Position Current-Voltage Relationships

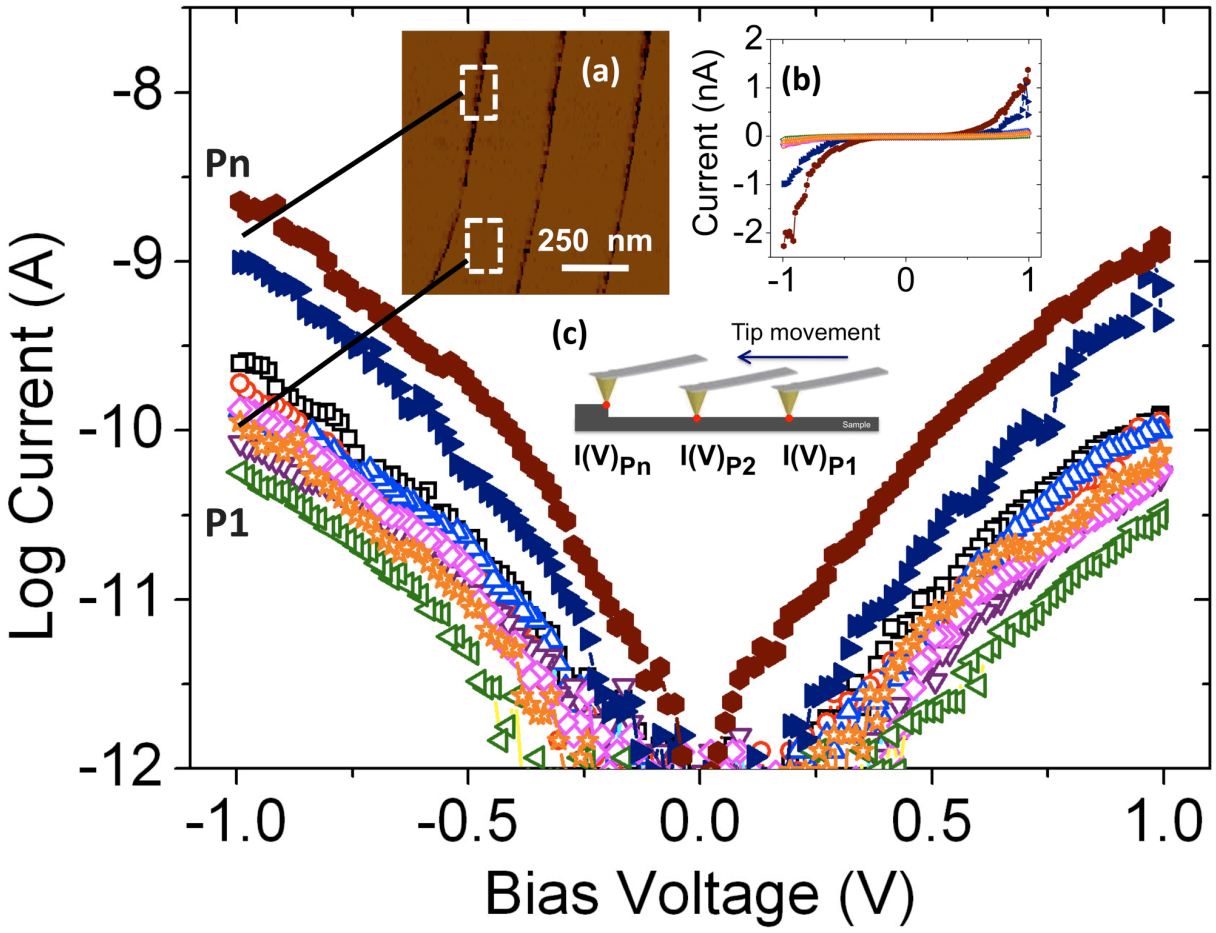

Fit to Thermionic Emission and Fowler-Nordheim Tunneling Models

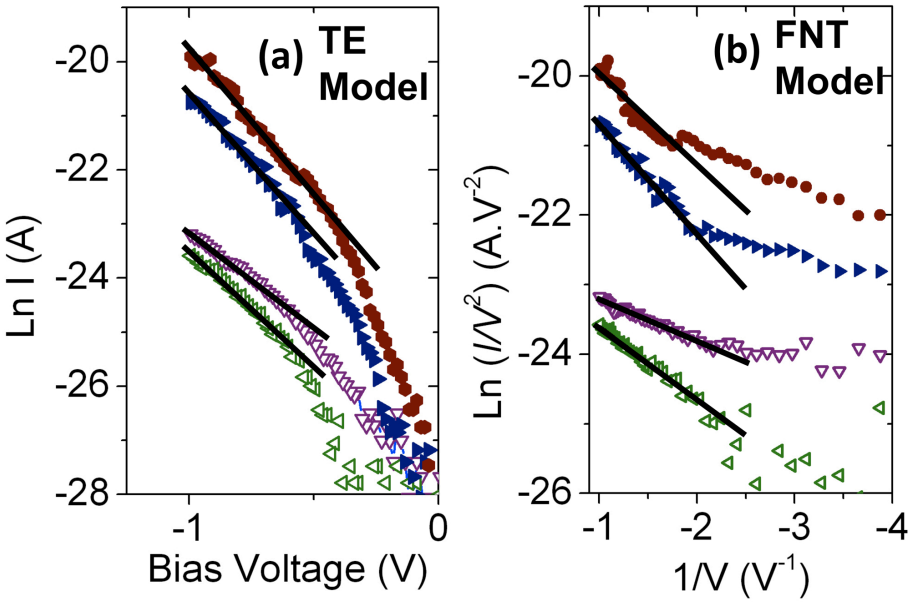

		Step -Edges			Terraces		
		Negative Bias	Positive Bias	Average	Negative Bias	Positive Bias	Average
TE	ϕ_B (eV)	0.283	0.316	**0.299±0.03**	0.338	0.365	**0.351±0.037**
	n	8.815	7.705	**8.260±1.76**	9.181	7.614	**8.397 ±1.89**
FNT	ϕ_B (eV)	0.795	0.951	**0.873±0.314**	0.790	0.959	**0.875±0.334**

Physical Mechanisms

- Geometric tip artifact
- Oxide, Contamination
- Physical damage
- Defect accumulation
- Strain: lateral force, edge-relaxation
- Dangling bonds, extended orbitals
- Topological protection

See:

Nanoscale Probing of Local Electrical Characteristics on MBE-Grown Bi_2Te_3 Surfaces under Ambient Conditions

Rita J. Macedo,[†] Sara E. Harrison,[‡] Tatiana S. Dorofeeva,[†] James S. Harris,[‡] and Richard A. Kiehl*,[†]

Macedo et al., *Nano Letters* 15, 4241-4247 (2015)

TI Step-Edge Transport Literature

Zhang et al., *Phys. Rev. Lett.* **2009,** 103, 266803.

STM and STS, voltage-dependent interference fringes at Bi_2Te_3 step edges, confirms suppressed backscattering.

Seo et al., *Nature* **2010,** 466, 343-346.

STM, transmission through terrace step-edges with high probability for the topological surface states on antimony.

Alpichshev et al., *Phys. Rev. Lett.* **2010,** 104, 016401.

STM of the DOS near a step-edge in Bi_2Te_3, 1D bound state in the bulk gap, bound to the step edge.

Deb et al., *J. Phys.: Condens. Matter* **2014,** 26, 315009.

Theory on 3D topological insulators, identified localized states that may propagate along step-edges, thereby providing an additional current path.

Kandala et al., *Nano Lett.* **2013**, 13, 2471.

Magnetotransport evidence of Aharonov−Bohm orbits around Bi_2Se_3 terraces, coherent scattering from step edges.

Magnetotransport Evidence of Terrace Step-Edge Channels

Surface-Sensitive Two-Dimensional Magneto-Fingerprint in Mesoscopic Bi_2Se_3 Channels

Abhinav Kandala, Anthony Richardella, Duming Zhang,[§] Thomas C. Flanagan, and Nitin Samarth*

The Center for Nanoscale Science and Department of Physics, The Pennsylvania State University, University Park, Pennsylvania 16802-6300, United States

Kandala et al., *Nano Lett*. 2013, 13, 2471−2476

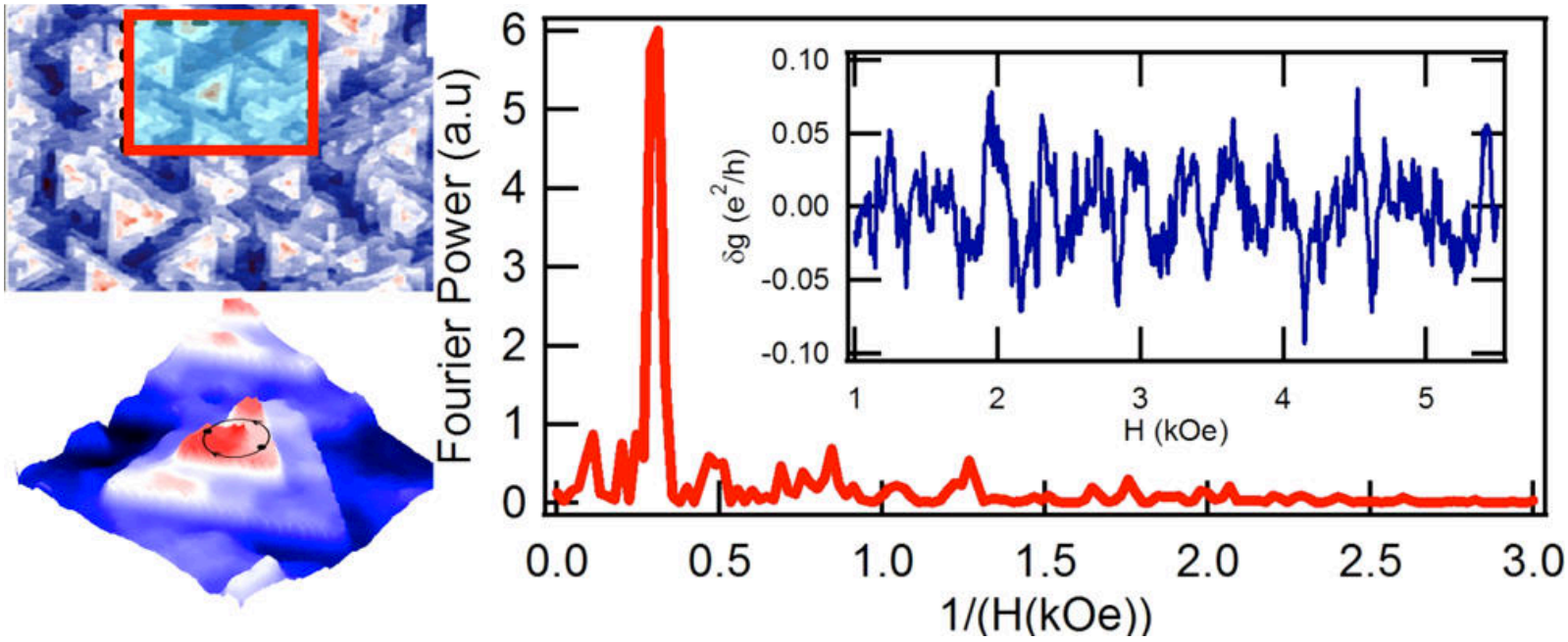

Possible Application:
Single Molecule Surface-Enhanced Raman Spectroscopy

Self-Assembled Ring Gratings

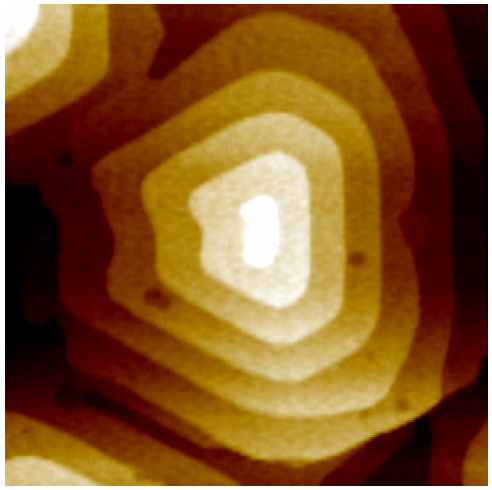

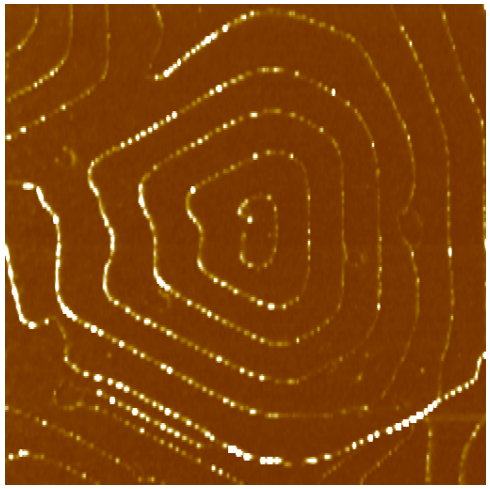

Vertical optical antennas integrated with spiral ring gratings for large local electric field enhancement and directional radiation

Baoan Liu,[1] Dongxing Wang,[2] Chuan Shi,[1] Kenneth B. Crozier,[2] and Tian Yang[1]*

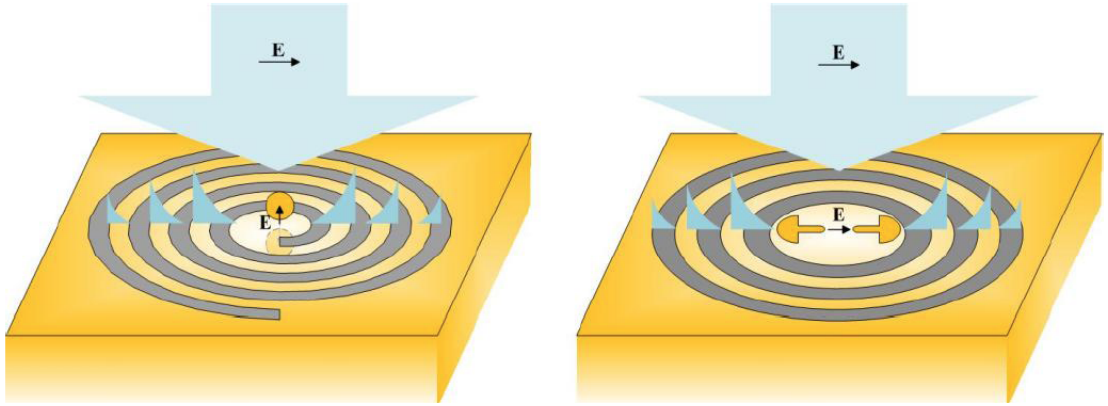

Liu et al, *Optics Express*, 19, 10049 (2011)

Self-Assembled Magnetic Nanoparticle Arrays Coupled to Surface Channels

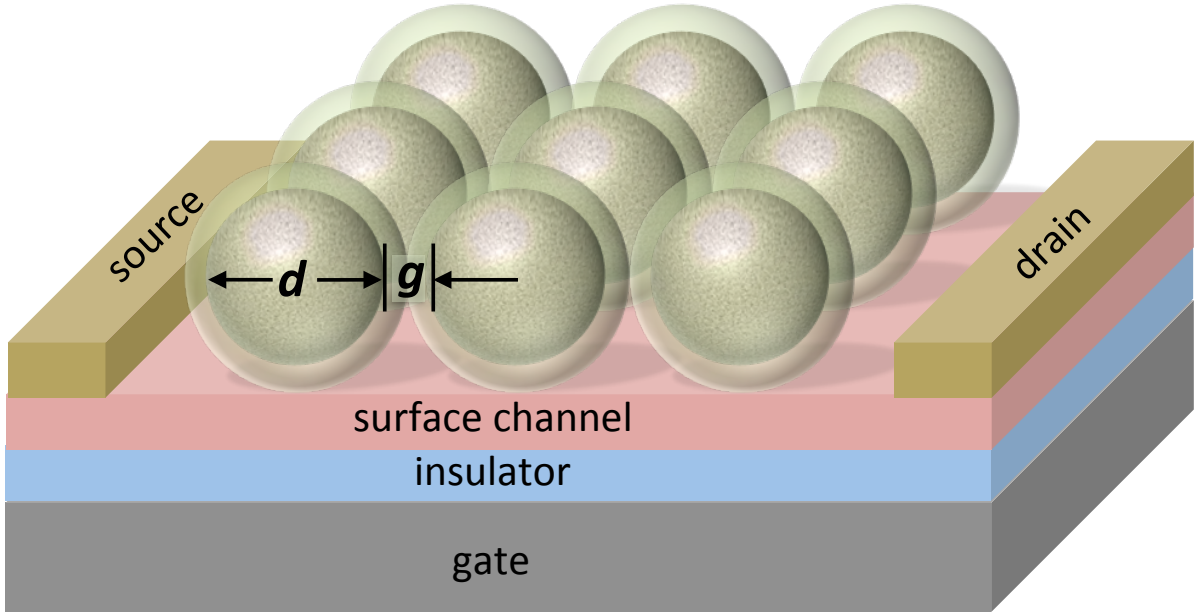

- **Nanoparticles**:
  - core composition
  - core diameter
  - spacer-shell thickness
- **Channels**:
  - graphene, MoS_2,
  - Bi_2Se_3
  - other TI
- **Device structures:**
  - NM contacts
  - FM contacts
  - back gate

Self-Assembled MNP Array on a Graphene Channel

18-nm Fe_3O_4 MNP with 1-nm oleic acid shells

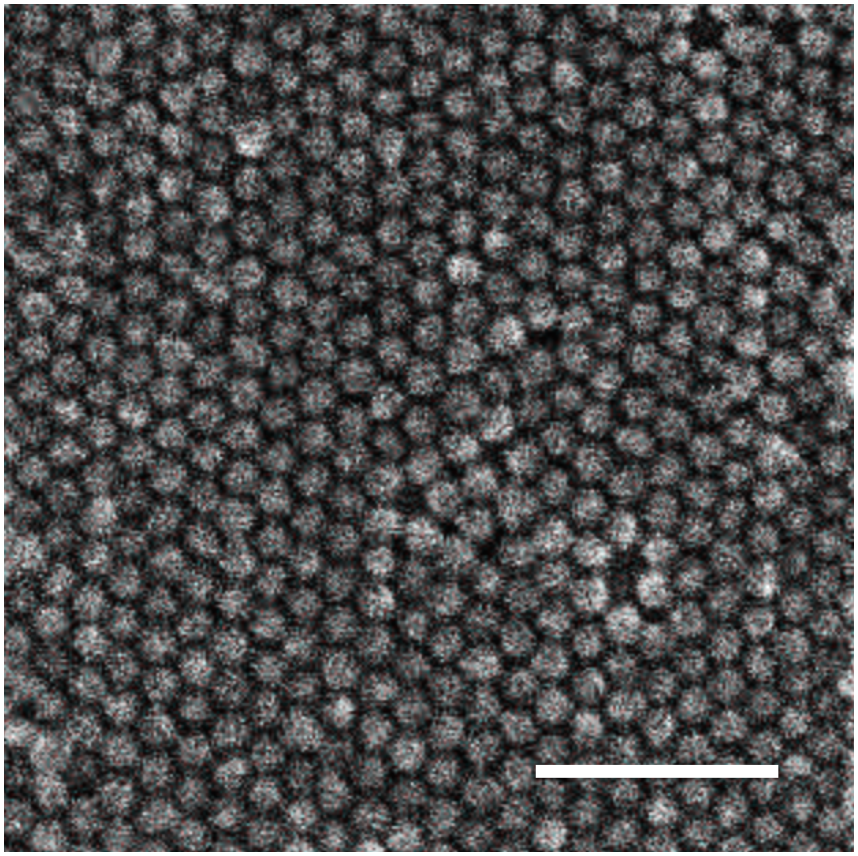

Scanning electron micrograph image.
(Scale bar 100-nm)

Current-AFM Confirmation of *Electronic* Coupling: Fe_3O_4 MNP to Graphene Channel

Topography (AFM)

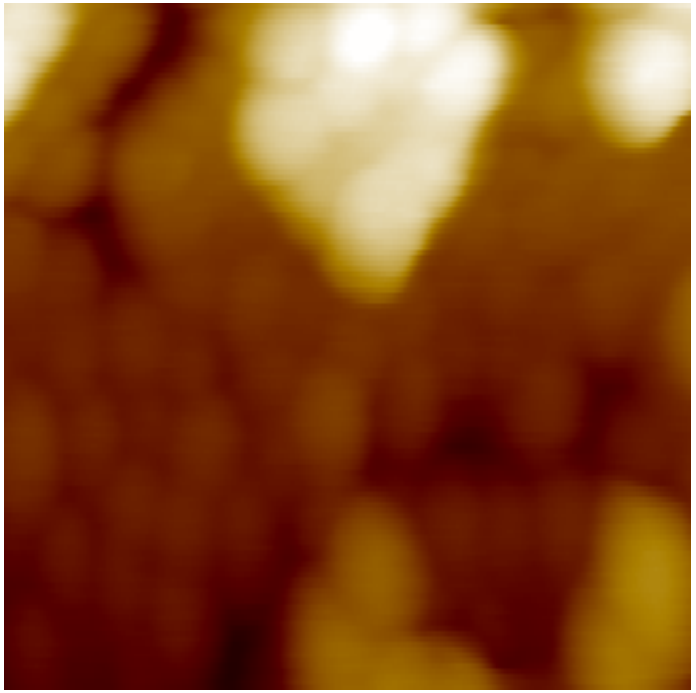

Current (C-AFM)

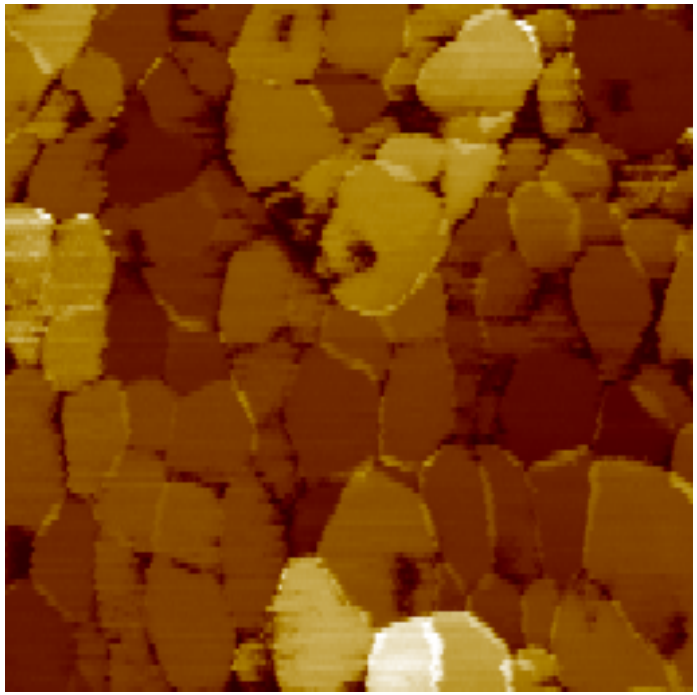

Hall Resistance for Fe_3O_4 MNP Array on Graphene as a Function of Gate Bias V_{gs}

Rxy vs H data showing nonlinearity at a field corresponding to the saturation field of the MNP array to be published.

Nonlinearities attributed to *anomalous Hall effect* (AHE)

AHE Component of Hall Resistance

R_{AHE} vs H data showing saturation at a field corresponding to the saturation field of the MNP array to be published.

AHE signature of *proximity induced ferromagnetism*

Magnetic Nanoparticle (MNP) Based Spin Torque Oscillator (STO) Arrays

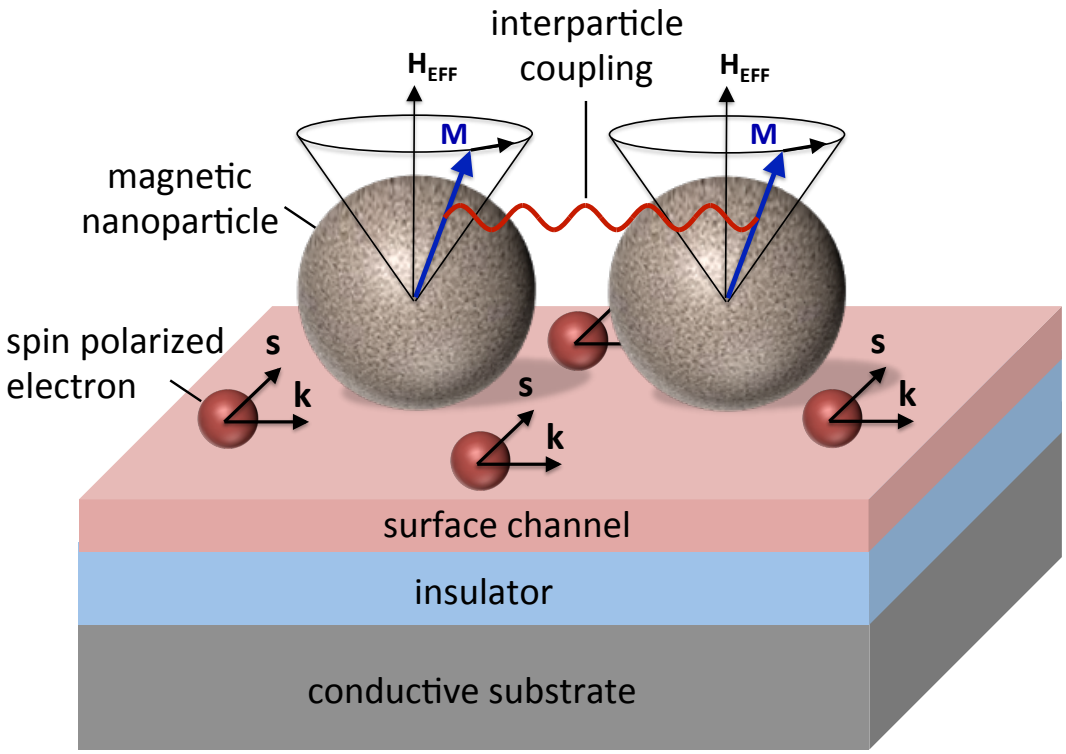

A spin polarized surface current drives magnetic precession in the MNPs by spin torque. Electronic and magnetic interparticle coupling mechanisms provide phase-locking of the oscillations.

Layout Advantage of MNP over Pillar MTJ STOs

Conventional MTJ STOs
with perpendicular current (CPP)

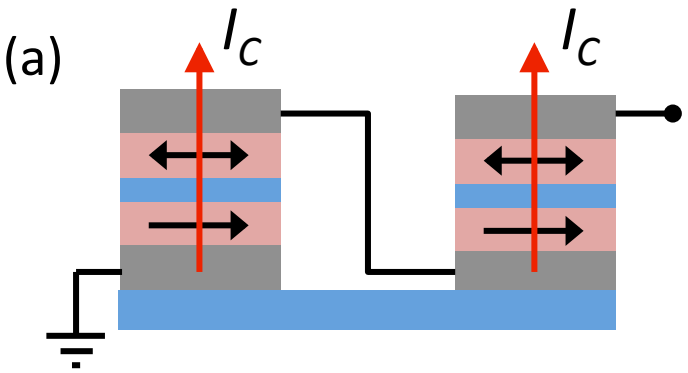

MNP STOs
with in-plane current (CIP)

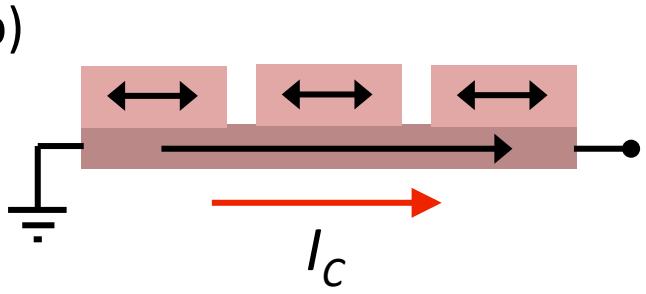

MNP STOs offer the advantage of simple, high density, series-connected structures.

Advantages of MNP STO Arrays

FEATURE	ADVANTAGE
small MNP → small *M* →	adequate STT with ultra-low I
nearly superparamagnetic →	
single crystal MNP → low loss → high Q →	robust to noise
CIP/GMR → low R → small V →	ultra-low power
self-assembled → high density →	scalable to massively parallel
tailorable MNP matl, size, spacing →	controllable *M* and coupling
lateral drive current → 2D layout →	simple fabrication
back-gate → global coupling control →	RF phase locking (pump ref)
optical input >→ control of local coupling →	2D data input

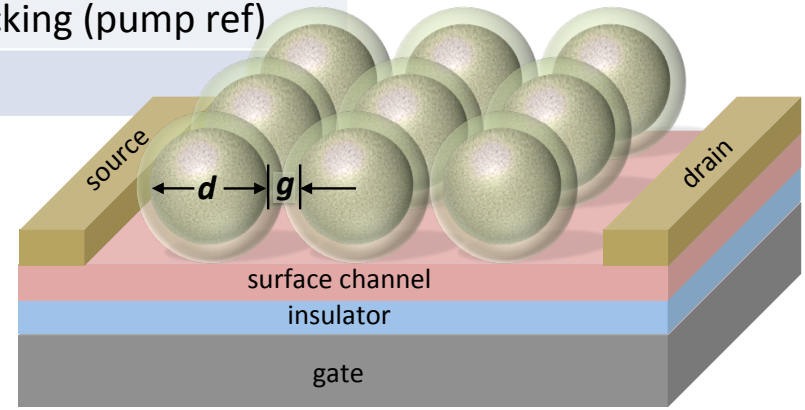

Information Processing with Oscillator Arrays

Tunneling Phase Logic

image processing function

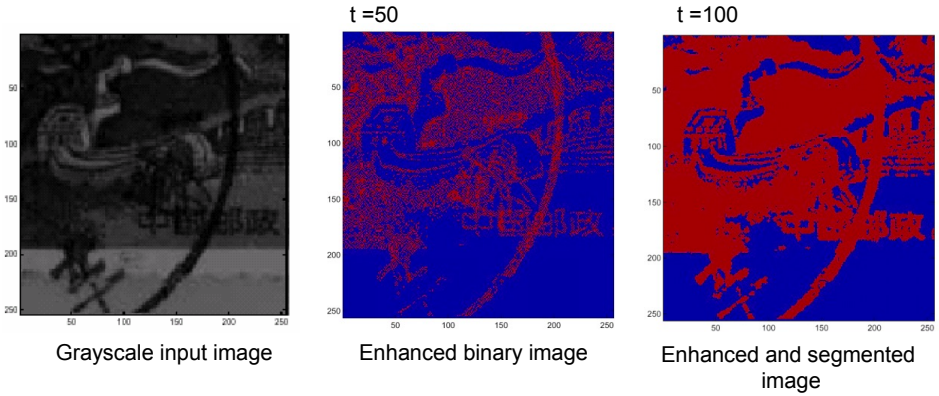

T. Yang, R. A. Kiehl, L. O. Chua, "Tunneling phase logic cellular nonlinear networks," Intl. J. Bifurcation and Chaos 11, 2895 (2001)

periodic pattern memory

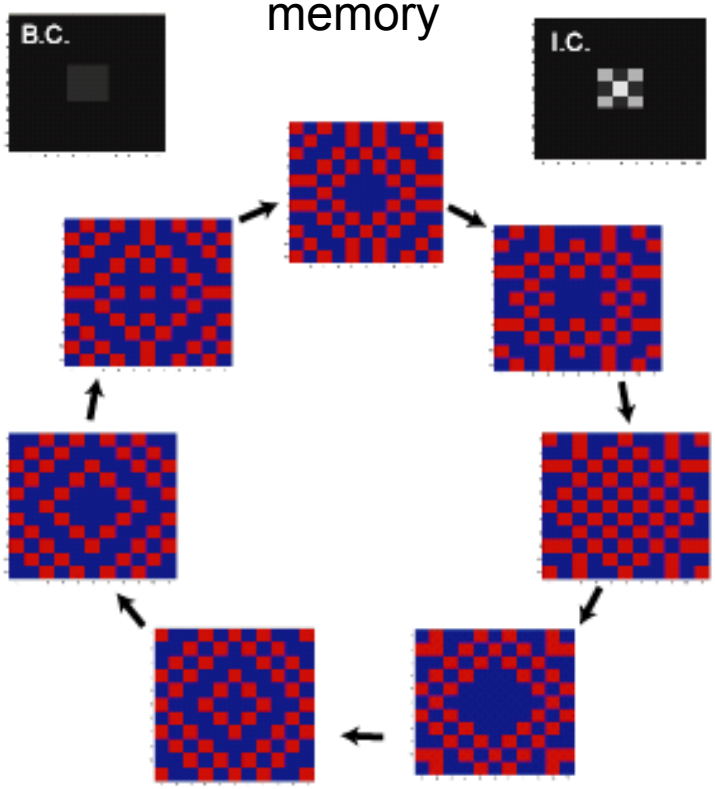

R.A. Kiehl, "Information Processing by Nonlinear Phase Dynamics in Locally Connected Arrays", *arXiv:1603.06665 [cs.NE]*.

Conclusion

Local Conductance Mapping of Terraced Bi_2Te_3 Surfaces

- Observe: 10 – 100X current enhancement at step edges
- Next: Topologically protected? Examine B-field and V_g effects
- Applications: SERS spectroscopy

Proximity Induced Ferromagnetism in Graphene from MNP Array

- Observe: AHE at 10 K for electrons and holes near Dirac point
- Next: V_g, T dependence; TI surface channels
- Applications: Energy efficient computing